Mixed Combustion Characteristics of Various Biomass Particles

Songying Zhao[*], Renfeng Wei

School of Municipal and Environmental Engineering, Jilin Jianzhu University, 130118 Changchun, China

[*] Correspondence: Songying Zhao (zhaosongying@jlju.edu.cn)

Abstract: As a promising pollutant emission reduction technology, biomass mixed combustion has attracted widespread attention worldwide. This paper aimed to study the characteristics of biomass mixed combustion and temperature distribution. A combination of simulation and experimental methods was adopted. The results showed when four kinds of biomass were burned separately, their highest temperatures in the center section of combustion chamber were corn stalk>cotton stalk>sawdust>rice straw in descending order. Compared with other three biomass, the highest temperature of corn stalk was more than 100 K higher, which mainly occurred during the full combustion stage, mainly because corn stalk had high volatile content and caught fire easily. In addition, with the optimal mixed combustion parameters, biomass mixed combustion improved the combustion characteristics of single biomass combustion. The optimal blending ratio of corn stalk to rice straw was 7:3, and the optimal primary air velocity and temperature were 48 m/s and 1300 K, respectively. With the optimal blending ratio, the maximum temperature in the center section was higher than that of single biomass combustion, with advanced ignition point, relatively uniform temperature distribution in the combustion chamber and good combustion performance, because the precipitation and combustion of high volatile components during mixed combustion caused the surface temperature of fixed carbon to rise rapidly to reach the ignition temperature. Finally, this paper studied the combustion characteristics of corn stalk and rice straw with the optimal mixed combustion parameters in mixed combustion experiment, and verified the good consistency between the simulation and experimental values. Therefore, biomass mixed combustion technology provides an important reference for solving the problem of low calorific value of single biomass combustion.

Keywords: Biomass energy; Mixed combustion characteristics; Numerical simulation; Temperature distribution

1. Introduction

As a clean, safe, sustainable, storable and environment-friendly new energy, biomass has attracted widespread attention at home and abroad [1]. Although China has various kinds of biomass from wide sources, the effective utilization rate is low, which not only wastes resources, but also does not comply with the national energy policies in the new era [2]. Compared with direct combustion technology, the research on biomass mixed combustion technology has great potential. Wang et al. [3-5] studied thermogravimetric analysis on biomass and coal mixed combustion, and analyzed the structural characteristics of samples using a Raman spectrometer. The research results showed that different structures of samples mainly caused significant differences in the combustion process, with the activation energy of biomass mixed combustion smaller than that of coal combustion, and the reactivity of biomass better than that of coal. Liao [6] studied the characteristics of pollutants released from coal and biomass mixed combustion, and the research results showed that the alkaline minerals contained in biomass effectively inhibited the release of NO and SO_2. Sousa et al. [7, 8] studied biomass particle mixed combustion models, and the research results showed that the commonly used particle mixed combustion models had shortcomings. They proposed to analyze the model index parameters required to simulate the conversion of single biomass particle, and pointed out that the mixed combustion models had more accurate requirements for the size of biomass particles. Yang et al. [9-11] studied the mixed combustion characteristics of biomass and coal. The research results showed that the increase of biomass blending ratio enhanced the volatility and reaction rate of the mixed fuel, and improved the characteristics of single fuel, such as combustion, burnout, pollutant emission, etc. Jia [12] studied the

combustion characteristics of five biomass particle fuels and analyzed their combustion kinetics. The results showed that the fuels had good combustion and kinetic characteristics. Li et al. [13] did systematic research on the physicochemical properties of biomass residue hydmchar (BRC) and Yangjing Pingding anthracite (YAC). The results showed that BRC addition to YAC improved the combustion performance, and significant synergistic effect occurred in the mixed combustion process.

The above scholars did research on the mixed combustion of biomass and coal. While few studies have investigated the characteristics of single biomass combustion, particularly the characteristics of biomass mixed combustion. Therefore, this paper studied the biomass mixed combustion. As a technology of efficient utilization of renewable clean energy, biomass mixed combustion not only improves the calorific value of fuel combustion, but also has good environmental benefits. Moreover, biomass substitutes fuel coal as a renewable clean, which greatly reduces the exploitation of non renewable resource coal. The development and utilization potential of biomass is significantly better than that of biomass and coal mixed combustion. The research results can provide certain guidance for the production and use of biomass fuel. This paper simulated the combustion of four kinds of biomass, namely, corn stalk, cotton stalk, sawdust, and rice straw, and mixed biomass in the combustion chamber using FLUENT software. Then this paper compared and analyzed the temperature distribution laws of the four biomass in the center section of combustion chamber. Finally this paper obtained the optimal mixed combustion parameters of the mixed biomass. This provides reference for the effective utilization of biomass resources, increase of biomass combustion efficiency and practical application of biomass in boiler combustion for power generation and heat supply.

2. Physical Model and Grid Partitioning

2.1 Physical Model

In order to study cylindrical combustion chamber boiler, this paper simplified the combustion chamber into a 10 m * 1 m two-dimensional pipe in accordance with the size and structural characteristics. Brief diagram of the combustion chamber physical model is shown in Figure 1. The two-dimensional pipe inlet has three kinds of air, and the primary air inlet is in the center of the pipe. Fuel particles enter the combustion chamber under the action of the primary air, and the inlet width is 0.25 m. Two kinds of air, upper and lower secondary air, enter the combustion chamber. The inlets are located on upper and lower sides of the primary air inlet, and are both 0.375 m wide. The upper and lower sides of the two-dimensional pipe are assumed to be wall surfaces. Industrial and elemental analysis of fuels is shown in Table 1.
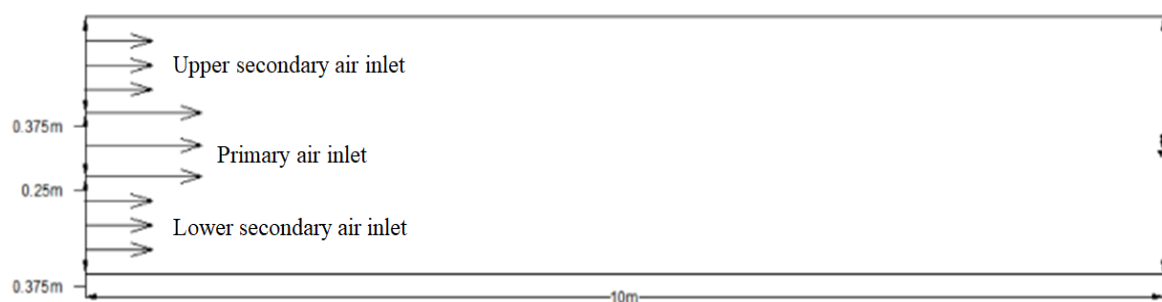

Figure 1. Brief diagram of the combustion chamber physical model

Table 1. Industrial and elemental analysis and calorific values of fuels

Fuel		Corn stalk	Cotton stalk	Sawdust	Rice straw
Industrial analysis/ (%)	Water content	4.89	5.03	5.25	8.86
	Ash content	5.07	8.52	4.38	13.62
	Volatile component	74.48	68.33	72.74	64.57
	Fixed carbon	15.56	18.12	17.63	12.95
Elemental analysis/ (%)	C	49.65	48.52	46.69	47.14
	H	6.36	5.85	5.65	5.42
	O	48.29	41.84	37.81	33.95
	N	0.85	0.69	0.34	0.32
	S	0.15	0.22	0.12	0.11
Calorific value/ MJ·kg^{-1}		17.432	15.527	14.286	13.375

2.2 Grid Partitioning

ICEM software was used for modeling and structured grid partitioning of the combustion chamber. The calculation area was partitioned into four kinds of grid quantity, 2×10^3, 3×10^3, 4×10^3 and 6×10^3, and the grid quality was checked respectively [14, 15]. It was found that grid quality reached above 0.99 in models with four kinds of grid quantity, indicating excellent quality. At the same time, the four models were calculated to verify the independence of the grids. According to comparative calculation, no significant changes occurred in the calculation results of models with grid quantity reaching 3×10^3, 4×10^3 and 6×10^3. Therefore, the model with 3×10^3 grid quantity was selected. The specific structured grid partitioning plot is shown in Figure 2.
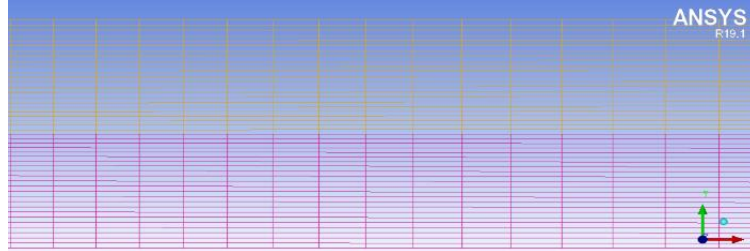

Figure 2. Local amplification plot of the structured grid

3. Boundary Conditions and Mathematical Model

3.1 Boundary Conditions

The inlet section of the three kinds of air in the combustion chamber was set as the velocity inlet boundary condition. The velocities of the three kinds of air and the flow rates of biomass particles were set according to the actual operating condition parameters of the boiler [16]. The size of biomass particles distributed regularly according to the Rosin-Rammler. Specific parameters set in boundary conditions are shown in Table 2. The combustion chamber outlet boundary condition was simplified, by setting the outlet boundary condition as pressure outlet, the upper and lower walls of the combustion chamber as adiabatic surfaces, and the wall surface as constant wall temperature [17].

Table 2. Parameters set in boundary conditions

Primary air velocity/	Upper and lower secondary air velocity/	Primary and secondary air temperature/	Pipe wall temperature/	Fuel mass flow rate/	Outlet temperature/	Density/	Particle size/
m/s	m/s	K	K	kg/s	K	kg/m³	μm
50	20	1500	1200	0.1	2000	1200	50

3.2 Mathematical Model

The mixed combustion of biomass fuels in combustion chamber is a complex physical and chemical process, involving multiple disciplines, such as multiphase fluid mechanics, heat and mass transfer, combustion, etc. [18]. In order to facilitate the study of the combustion performance of mixed biomass, this paper calculated the air flow in the combustion chamber as steady state, while taking into consideration the effect of gravity. Therefore, this paper calculated gas phase turbulent transport in the simulation calculation using standard k-ε turbulence model. The general equation was as follows [19]:

$$\text{div}pv\varphi = div\Gamma_\Phi \nabla\varphi + S_\varphi \tag{1}$$

where, P is the air density, v is the velocity component, ϕ is a general variable, Γ_Φ is the transport coefficient, and S_φ is the air source term.

This paper simulated the mixed combustion of biomass fuels in combustion chamber using FLUENT software, calculated gas phase turbulent transport in simulation calculation using k-ε turbulence model, simulated the flow of fuel particles using Discrete Phase Model (DPM), calculated the radiation heat transfer process using P1 radiation model, and simulated gas phase turbulence mixed combustion using the dual mixed probability density function model [20]. Second order upwind scheme with high accuracy was selected for the discrete scheme and Semi-Implicit Method for Pressure Linked Equations (SIMPLE) algorithm was used for calculation [21].

4. Single Biomass Combustion Simulation Results and Analysis

Figure 3 is temperature distribution nephogram in the center section of combustion chamber during the combustion of four kinds of biomass. As shown in the figure, the highest temperatures in the center section of combustion chamber during the combustion of four kinds of biomass are corn stalk>cotton stalk>sawdust>rice straw in descending order, which are 2010 K, 1910 K, 1880 K, and 1830 K, respectively. The highest temperature in the center section during the combustion of corn stalk was more than 100 K higher than that of other three kinds of biomass, and 180 K higher than that of rice straw, which was basically consistent with the calorific values of the three biomass, indicating that the maximum temperature of biomass fuel with high calorific value in the center section was higher than that of biomass fuels with low calorific values. Simulation results showed that the high temperature regions in the center section concentrated in the middle and rear of the combustion chamber during the single combustion of three kinds of biomass. It was analyzed that the three kinds of biomass were quickly transported to the entire combustion chamber because of their small density and easy entrainment by the primary air flow, indicating that the combustion performance of biomass was greatly affected by the primary air velocity. Compared with other three kinds of biomass, corn stalk had earlier ignition point and enlarged high-temperature areas, with a relatively uniform temperature distribution throughout the combustion chamber, because corn stalk had high volatile content and caught fire easily. Although sawdust had similar volatile content to corn stalk, its calorific value was low, therefore, the high-temperature area of sawdust was smaller than that of corn stalk. As a result, the mixed combustion of cotton stalk, sawdust, rice straw and corn stalk in a certain proportion can improve the performance of combustion.
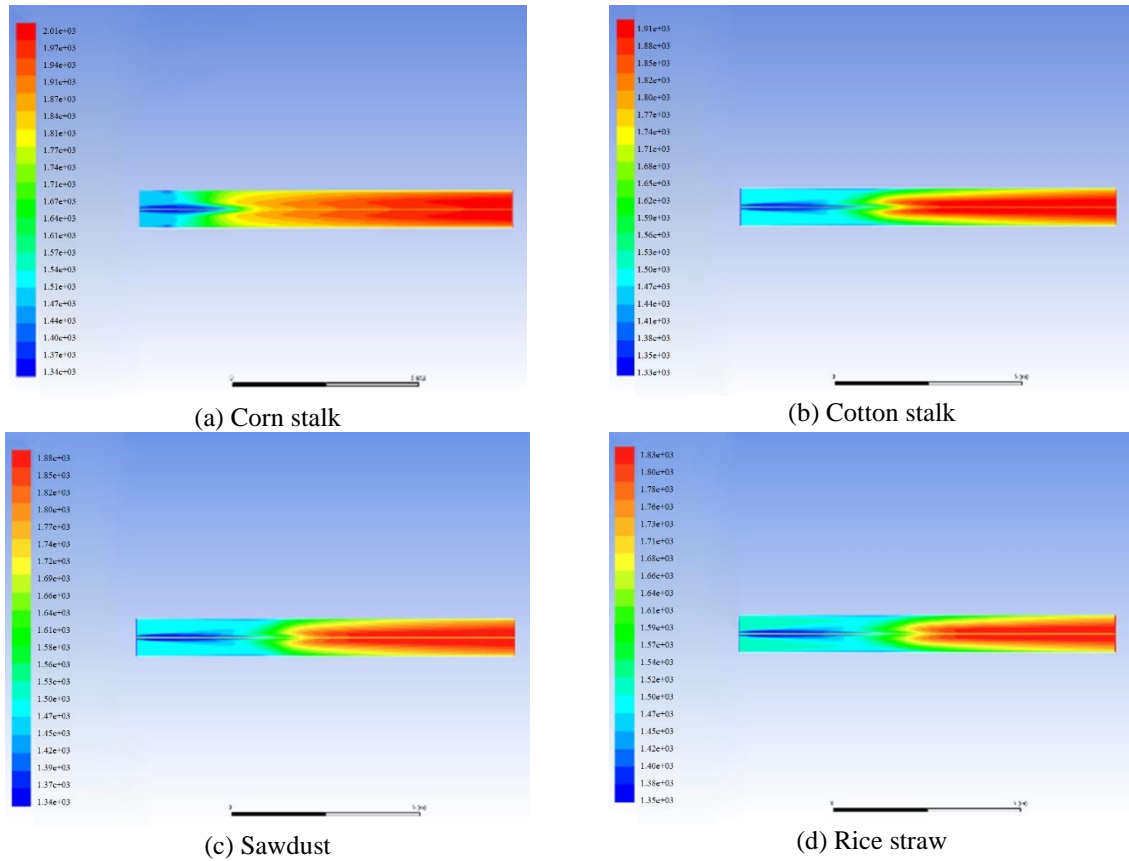

(a) Corn stalk

(b) Cotton stalk

(c) Sawdust

(d) Rice straw

Figure 3. Temperature distribution nephogram in the center section of combustion chamber during combustion of four kinds of biomass (unit: K)

Figure 4 shows change curve of the center section temperature along with the combustion chamber position during single biomass combustion. As shown in the figure, the first stage during combustion of four biomass fuels was dehydration and drying, where temperature between 0 and 2 m in the combustion chamber was above 1300 K. But temperature in the center section showed a downward trend, because the primary air temperature at the combustion chamber inlet was relatively high. When the fuel was transported into the combustion chamber, it was not completely burned, which caused the downward temperature trend in the combustion chamber. In the second stage of full combustion, as the fuel fully combusted, the center section temperature between 2 and 7 m in the combustion chamber rapidly increased. However, the temperature of corn stalk was significantly higher than that

of other three biomass fuels within this range, because lower moisture content of corn stalk caused faster combustion speed and higher temperature. In the third stage, as the calorific values of fuels gradually decreased, the center section temperature between 7 and 10 m in the rear section of combustion chamber presented a downward trend. Due to high calorific value, the center section temperature of corn stalk decreased significantly differently from other three biomass fuels. Therefore, the combustion performance of biomass was affected by both air temperature and water content.
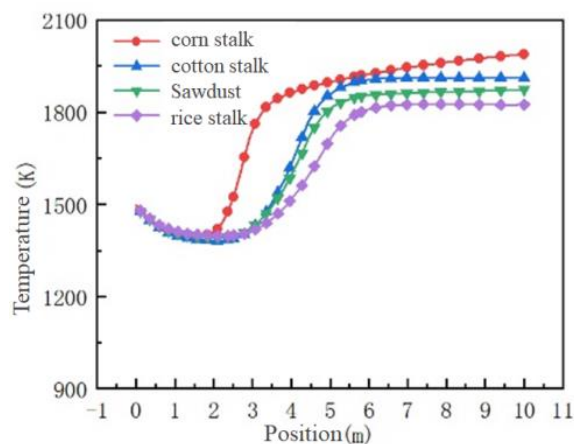

Figure 4. Change curve of center section temperature with the combustion chamber position during single combustion of four kinds of biomass

5. Mixed Combustion Simulation Results and Analysis

Combined with the numerical simulation results of single biomass combustion, corn stalk and rice straw, which had the highest and the lowest temperature in the center section of combustion chamber, were selected for mixed combustion simulation with different blending ratios, primary air velocities and temperatures. The corresponding effects on the temperature field in the center section of combustion chamber were analyzed in order to obtain the optimal mixed combustion parameters.

5.1 Different Blending Ratios

Corn stalk and rice straw, which had the highest and the lowest center section temperature in the combustion chamber, were used for mixed combustion simulation with different blending ratios of 4:1, 3:1, 7:3 and 3:2. After analyzing the impact of different blending ratios on the temperature field in the combustion chamber, this paper obtained the optimal blending ratio for biomass mixed combustion. The results are shown in Figure 5.
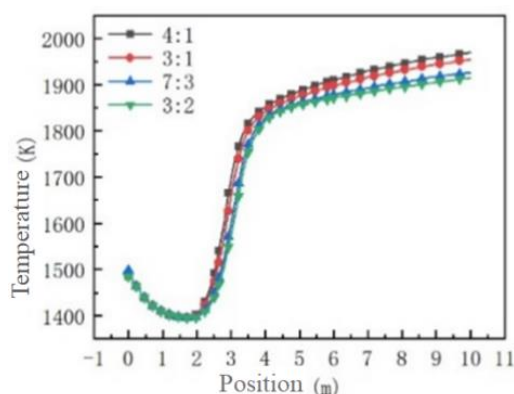

Figure 5. Temperature distribution in center section of combustion chamber in mixed combustion of corn stalk and rice straw with different blending ratios

Figure 5 shows the simulated temperature values in the center section of combustion chamber in mixed combustion of corn stalk and rice straw with different blending ratios. As shown in the figure, the maximum temperatures in the center section with four blending ratios are 1951 K, 1938 K, 1922 K, and 1892 K, respectively.

With increased blending ratio of rice straw, the maximum temperature in the central section presented a downward trend. When the blending ratio was 4:1 and 3:1, the maximum temperature variation trend in the center section was not obvious. The maximum temperature variation trend in the center section decreased significantly when the ratio was greater than 7:3 and began to decrease when the ratio was 3:2. Therefore, the optimal blending ratio of corn stalk to rice straw was 7:3, which had advanced ignition point, an increase of the maximum temperature in the center section by 92 K, expanded high-temperature regions and relatively uniform temperature distribution in the combustion chamber, compared with combustion of rice straw alone.

5.2 Different Primary Air Velocities

Corn stalk and rice straw, which had the highest and the lowest center section temperature in the combustion chamber, were used for mixed combustion simulation at different primary air velocities of 44 m/s, 46 m/s, 48 m/s, 50 m/s, 52 m/s, and 54 m/s, respectively. After analyzing the impact of different primary air velocities on the temperature field in the combustion chamber, this paper obtained the optimal primary air velocity for biomass mixed combustion. The results are shown in Figure 6.
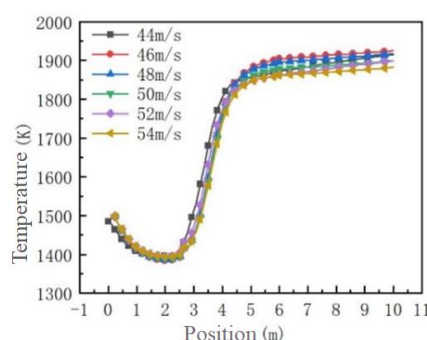

Figure 6. Temperature distribution in the center section of combustion chamber in mixed combustion of corn stalk and rice straw at different primary air velocities

Figure 6 shows the temperature distribution diagram in the center section of combustion chamber in mixed combustion of corn stalk and rice straw at different primary air velocities. As shown in the figure, the overall trend of temperature change in the center section does not change along with the change of primary air velocity. Temperature in the central section showed an upward trend at 44-46 m/s primary air velocity, and showed a downward trend at 48-54 m/s primary air velocity. It can be seen that the lower the primary air velocity, the more beneficial to the mixed combustion, because lower primary air velocity causes the fuels to stay longer in the combustion chamber, which enables the mixed fuel to fully combust. However, it does not mean that the lower the velocity, the better, because decreased primary air velocity easily leads to insufficient air volume in the combustion chamber, resulting in insufficient combustion of the mixed fuel and reducing heat release. Increased primary air velocity shortens the residence time of the mixed fuel in the combustion chamber, which causes the mixed fuel to not fully combust and delays the ignition point. At the same time, it can be seen that the maximum center section temperature in combustion chamber is closer to the combustion chamber outlet. Therefore, the optimal primary air velocity for biomass mixed combustion is 48 m/s.

5.3 Different Primary Air Temperatures

Corn stalk and rice straw, which had the highest and the lowest center section temperature in the combustion chamber, were used for mixed combustion simulation at different primary air temperatures of 1000 K, 1100 K, 1200 K, 1300 K, 1400 K, and 1500 K. After analyzing the impact of different primary air temperatures on the temperature field in the combustion chamber, this paper obtained the optimal primary air temperature for biomass mixed combustion. The results are shown in Figure 7.

Figure 7 is temperature distribution diagram of the center section of combustion chamber in mixed combustion of corn stalk and rice straw at different primary air temperatures. As shown in the figure, the combustion is relatively intense near the 2-4 m section, and the temperature rises rapidly. Moreover, due to heat exchange with air and decrease in calorific value of the fuel during the later combustion stage, the temperature near the 5-10 m section at the rear of the combustion chamber becomes lower. It can be seen from the figure that with the change of primary air temperature, the overall trend of temperature change in the center section does not change. In addition, with the increase of primary air temperature, the temperature in the center section presents an upward trend. However, when the air temperature is greater than 1300 K, the upward temperature trend in the center section gradually decreases. It can be seen from the figure that primary air temperature is inversely proportional to ignition

time, that is, the higher the supply air temperature, the shorter the ignition time, because higher supply air temperature makes the heating rate of the mixed fuel faster and the required ignition time shorter. It can be seen that the higher the primary air temperature, the more beneficial to mixed combustion. However, it does not mean that the higher the primary air temperature, the better. Too high air temperature reduces the heat transfer temperature difference of the air preheater, resulting in a decrease in heat transfer. Although it improves the combustion temperature of the combustion chamber and the mixed combustion effects, it also increases the flue gas temperature in the combustion chamber, ultimately leading to an increase in the exhaust gas temperature, thus reducing the thermal efficiency of boiler. Therefore, the optimal primary air temperature for biomass mixed combustion is 1300 K.
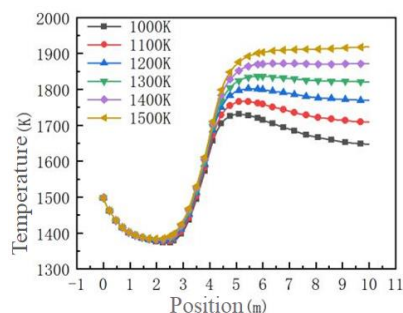

Figure 7. Temperature distribution in center section of combustion chamber in mixed combustion of corn stalk and rice straw at different primary air temperatures

6. Mixed Combustion Experiment

6.1 Experiment Content

This paper mixed 70% corn stalk and 30% rice straw fuel using a small processing equipment and uniformly sent them into the combustion chamber for mixed combustion using primary air at 1300 K air temperature, aiming to verify the optimal mixed combustion parameters of corn stalk and rice straw with 7:3 blending ratio at 1300 K primary air temperature and 48 m/s primary air velocity, thus improving the combustion characteristics of single biomass.

6.2 Experimental Method

The working conditions set in experiment are shown in Table 3. With air as the working atmosphere, mixed biomass particles were uniformly sent into the combustion chamber through primary air for mixed combustion. A B-type thermocouple temperature monitoring point was set every one meter on the wall surface of combustion chamber, which was used to record the temperature on the combustion chamber wall. Figure 8 is a schematic diagram of the combustion chamber wall temperature monitoring points.

Table 3. Experimental conditions

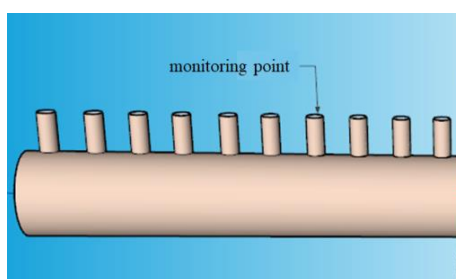| Biomass fuel	Primary air velocity/(m/s)	Secondary air velocity/(m/s)	Powder feeding amount/(kg/h）	Composite biomass ratio	Notes
Corn stalk: rice straw	48	20	360	7:3	Mixed combustion

Figure 8. Schematic diagram of combustion chamber temperature monitoring points

Due to combustion characteristics of mixed fuels, a small combustion chamber test bench was used (Figure 9), including air supply device, temperature control heating system, combustion chamber, and temperature measurement system.
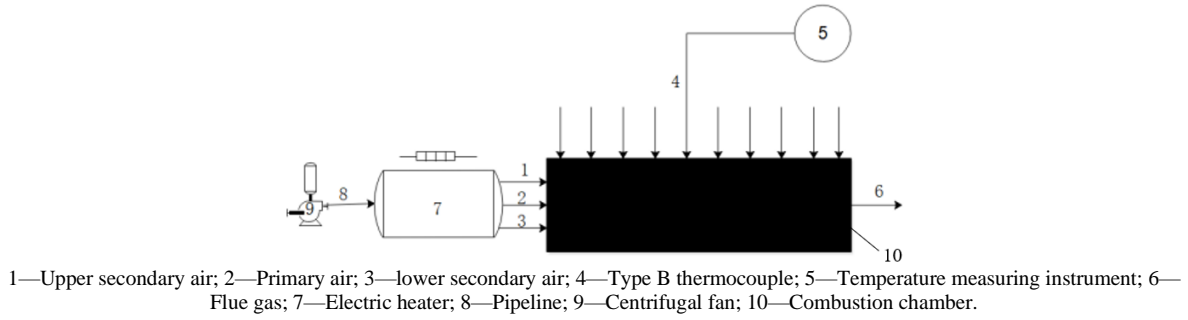

1—Upper secondary air; 2—Primary air; 3—lower secondary air; 4—Type B thermocouple; 5—Temperature measuring instrument; 6—Flue gas; 7—Electric heater; 8—Pipeline; 9—Centrifugal fan; 10—Combustion chamber.

**Figure 9.** Schematic diagram of small combustion chamber test bench

6.3 Experiment Results and Analysis

Wall temperature variation in the combustion chamber of corn stalk and rice straw mixed combustion is shown in Figure 10. Under the working conditions of optimal blending ratio, optimal primary air velocity and temperature, both the experimental and simulated values of combustion chamber wall temperature reached the maximum value.

Figure 10 shows the contrastive analysis of simulated and experimental values of the maximum temperature in the center section under the working conditions of 7:3 optimal blending ratio of corn stalk to rice straw in Figure 10(a), 48 m/s primary air velocity in Figure 10(b), and 1300 K primary air temperature in Figure 10(c). As shown in the figure, the simulated and experimental values are well consistent. Therefore, the above model can be used to verify the calculation and prediction of temperature distribution in the combustion chamber, with corn stalk and rice straw under different parameter conditions.
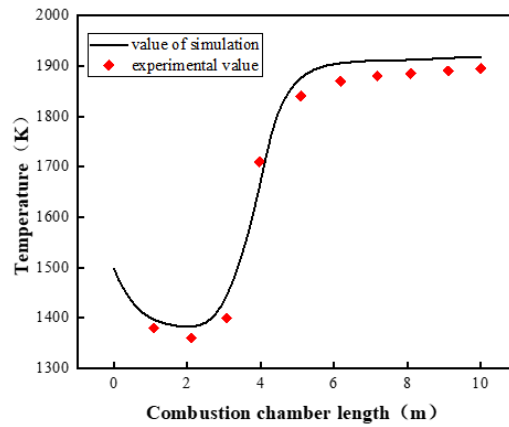
(a) Optimal blending ratio
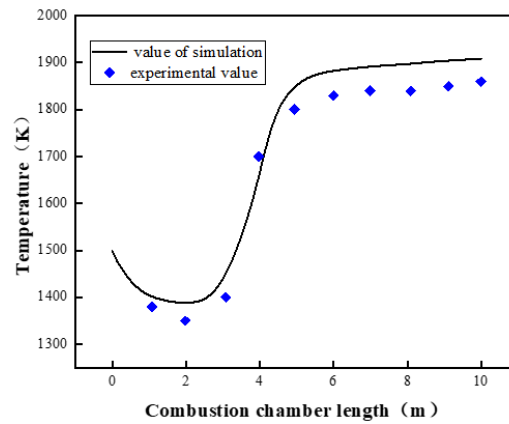
(b) Optimal primary air velocity
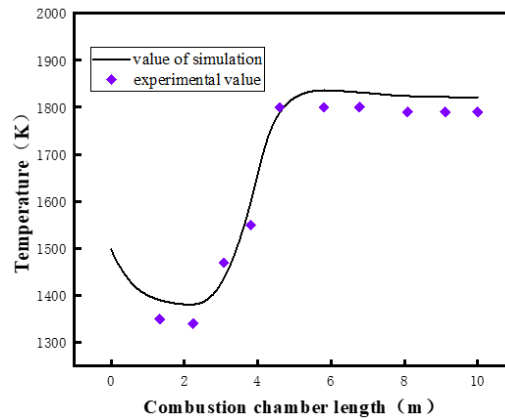
(c) Optimal primary air temperature

Figure 10. Comparison of simulated and experimental values of corn stalk and rice straw with optimal parameters

7. Conclusion

This paper simulated single and mixed combustion of four kinds of biomass using FLUENT software, and obtained the temperature distribution of different biomass in the center section of combustion chamber, the factors influencing the characteristics of biomass mixed combustion, and the optimal mixed combustion parameters of corn stalk and rice straw. The following conclusions were obtained:

(1) The maximum temperatures of biomass fuels with high calorific values in the center section of combustion chamber were higher than those of biomass fuels with low calorific values. The maximum temperatures of corn stalk, cotton stalk, sawdust, and rice straw in the center section were 2010 K, 1910 K, 1880 K, and 1830 K, respectively. Compared with other three kinds of biomass, corn stalk had earlier ignition point during combustion, expanded high-temperature regions, and relatively uniform temperature distribution in the combustion chamber;

(2) With the optimal blending ratio, the maximum temperature of mixed combustion in the center section of combustion chamber was 92 K higher than that of single combustion. In addition, the mixed combustion had advanced temperature increase and ignition point, relatively uniform temperature distribution in the combustion chamber, and good combustion performance.

(3) The characteristics of biomass mixed combustion were greatly influenced by blending ratio, primary air velocity, and primary air temperature. With the optimal mixed combustion parameters, biomass mixed combustion improved the combustion performance of single biomass combustion.

(4) Experiment showed that corn stalk mixed with 30% rice straw changed the combustion characteristics of mixed fuel particles, which increased the temperature of single fuel combustion to 1922 K. In addition, this completed the simulation and experimental verification of key processes in the mixed combustion technology of corn stalk and rice straw, which had the highest and the lowest center section temperature in the combustion chamber, laying a foundation for the industrial application and promotion of this technology.

Data Availability

The data used to support the findings of this study are available from the corresponding author upon request.

Conflicts of Interest

The authors declare that they have no conflicts of interest.

References

[1] Q. Y. Zhang, Y. X. Liu, Y. H. Cao, Z. Y. Li, J. C. Hou, and X. Gou, "Parametric study and optimization of MEA-based carbon capture for a coal and biomass co-firing power plant," *Renew Energy*, vol. 205, pp. 838-

850, 2023. https://doi.org/10.1016/j.renene.2022.12.099.

[2] J. X. Guo, "Retrofitting strategy for biomass co-fired power plant," *Clean Techn. Environ Policy*, vol. 24, no. 8, pp. 2531-2545, 2020. https://doi.org/10.1007/s10098-022-02332-y.

[3] Q. Wang, G. W. Wang, J. L. Zhang, J. Y. Lee, H. Y. Wang, and C. Wang, "Combustion behaviors and kinetics analysis of coal, biomass and plastic," *Thermochim Acta*, vol. 669, pp. 140-148, 2018. https://doi.org/10.1016/j.tca.2018.09.016.

[4] P. Wang, G. W. Wang, J. L. Zhang, J. Y. Lee, Y. J. Li, and C. Wang, "Co-combustion characteristics and kinetic study of anthracite coal and palm kernel shell char," *Appl Therm Eng.*, vol. 143, pp. 736-745, 2018. https://doi.org/10.1016/j.applthermaleng.2018.08.009.

[5] G. W. Wang, J. L. Zhang, J. G. Shao, Z. J. Liu, G. H. Zhang, T. Xu, J. Guo, H. Y. Wang, R. S. Xu, and H. Lin, "Thermal behavior and kinetic analysis of co-combustion of waste biomass/low rank coal blends," *Energy Convers. Manage.*, vol. 124, pp. 414-426, 2016. https://doi.org/10.1016/j.enconman.2016.07.045.

[6] X. J. Liao, S. H. Zhang, X. C. Wang, J. N. Shao, X. Zhang, X. H. Wang, H. P. Yang, and H. P. Chen, "Co-combustion of wheat straw and camphor wood with coal slime: Thermal behaviour, kinetics, and gaseous pollutant emission characteristics," *Energy*, vol. 234, Article ID: 121292, 2021. https://doi.org/10.1016/j.energy.2021.121292.

[7] N. Sousa and J. L. T. Azevedo, "Model simplifications on biomass particle combustion," *Fuel*, vol. 184, pp. 948-956, 2016. https://doi.org/10.1016/j.fuel.2016.03.106.

[8] H. Kovacs, K. Szemmelveisz, and T. Koós, "Theoretical and experimental metals flow calculations during biomass combustion," *Fuel*, vol. 185, pp. 524-531, 2016. https://doi.org/10.1016/j.fuel.2016.08.007.

[9] X. D. Yang, Z. Y. Luo, X. R. Liu, C. J. Yu, Y. A. Li, and Y. C. Ma, "Experimental and numerical investigation of the combustion characteristics and NO emission behaviour during the co-combustion of biomass and coal," *Fuel*, vol. 287, Article ID: 119383, 2021. https://doi.org/10.1016/j.fuel.2020.119383.

[10] B. Q. Ye, R. Zhang, J. Cao, K. Lei, and D. Liu, "The study of co-combustion characteristics of coal and microalgae by single particle combustion and TGA methods," *J. Energy Inst.*, vol. 93, no. 2, pp. 508-517, 2020. https://doi.org/10.1016/j.joei.2019.07.001.

[11] K. L. Cong, F. Han, Y. G. Zhang, and Q. H. Li, "The investigation of co-combustion characteristics of tobacco stalk and low rank coal using a macro-TGA," *Fuel*, vol. 237, pp. 126-132, 2019. https://doi.org/10.1016/j.fuel.2018.09.149.

[12] G. H. Jia, "Combustion characteristics and kinetic analysis of biomass pellet fuel using thermogravimetric analysis," *Processes*, vol. 9, no. 5, pp. 868-868, 2021. https://doi.org/10.3390/pr9050868.

[13] J. H. Li, R. S. Xu, G. W. Wang, J. L. Zhang, B. Song, W. Liang, and C. Wang, "Study on the feasibility and co-combustion mechanism of mixed injection of biomass hydrochar and anthracite in blast furnace," *Fuel*, vol. 304, Article ID: 121465, 2021. https://doi.org/10.1016/j.fuel.2021.121465.

[14] A. M. García, M. Alejandro Rendon, and A. A. Amell, "Combustion model evaluation in a CFD simulation of a radiant-tube burner," *Fuel*, vol. 276, Article ID: 118013, 2020. https://doi.org/10.1016/j.fuel.2020.118013.

[15] C. S. Bu, G. Alberto, L. Bo, X. Y. Wang, J. B. Zhang, and G. L. Piao, "The effect of H_2O on the oxy-fuel combustion of a bituminous coal char particle in a fluidized bed: Experiment and modeling," *Combust. Flame*, vol. 218, pp. 42-56, 2020. https://doi.org/10.1016/j.combustflame.2020.03.025.

[16] X. X. Meng, T. M. Ismail, W. Zhou, Y. H. Yan, X. H. Ren, R. Sun, and M. Abd El-Salam, "Numerical study of preheating primary air on pinewood and corn straw co-combustion in a fixed bed using Eulerian-Eulerian approach," *Fuel*, vol. 289, Article ID: 119455, 2021. https://doi.org/10.1016/j.fuel.2020.119455.

[17] J. Collazo, J. Porteiro, J. L. Míguez, E. Granada, and M. A. Gómez, "Numerical simulation of a small-scale biomass boiler," *Energy Convers. Manage.*, vol. 64, pp. 87-96, 2012. https://doi.org/10.1016/j.enconman.2012.05.020.

[18] X. B. Wang, J. Y. Zhang, X. W. Xu, H. Mikulčić, Y. Li, Y. G. Zhou, and H. Z. Tan, "Numerical study of biomass Co-firing under Oxy-MILD mode," *Renew Energy*, vol. 146, pp. 2566-2576, 2020. https://doi.org/10.1016/j.renene.2019.08.108.

[19] R. Chen, Y. Rao, H. H. Yue, Y. Ai, X. Zhang, L. L. Zhang, and J. X. Zhang, "Numerical simulation of bed combustion in biomass-briquette boiler," *J. Energy Eng.*, vol. 146, no. 4, Article ID: 04020031, 2020. https://doi.org/10.1061/(ASCE)EY.1943-7897.0000653.

[20] P. Madejski, "Numerical study of a large-scale pulverized coal-fired boiler operation using CFD modeling based on the probability density function method," *Appl Therm Eng.*, vol. 145, pp. 352-363, 2018. https://doi.org/10.1016/j.applthermaleng.2018.09.004

[21] T. B. Gu, W. B. Ma, Z. N. Guo, T. Berning, and C. G. Yin, "Stable and clean co-combustion of municipal sewage sludge with solid wastes in a grate boiler: A modeling-based feasibility study," *Fuel*, vol. 328, Article ID: 125237, 2022. https://doi.org/10.1016/j.fuel.2022.125237.